SYSTEM ANALYSIS OF *PHYCOMYCES* LIGHT-GROWTH RESPONSE

Photoreceptor and Hypertropic Mutants

ANURADHA PALIT, PROMOD PRATAP, AND EDWARD D. LIPSON
Department of Physics, Syracuse University, Syracuse, New York 13244-1130

ABSTRACT The light-growth responses of *Phycomyces* behavioral mutants, defective in genes *madB*, *madC*, and *madH*, were studied with the sum-of-sinusoids method of system identification. Modified phototropic action spectra of these mutants have indicated that they have altered photoreceptors (P. Galland and E. D. Lipson, 1985, *Photochem. Photobiol.* 41:331). In the two preceding papers, a kinetic model of the light-growth response system was developed and applied to wild-type frequency kernels at several wavelengths and temperatures. The present mutant studies were conducted at wavelength 477 nm. The log-mean intensity was 6×10^{-2} W m^{-2} for the *madB* and *madC* night-blind mutants, and 10^{-4} W m^{-2} for the *madH* hypertropic mutant. The prolonged light-growth responses of the *madB* and *madC* mutants are reflected in the reduced dynamic order of their frequency kernels. The linear response of the hypertropic mutant is essentially normal, but its nonlinear behavior shows modified dynamics. The behavior of these mutants can be accounted for by suitable modifications of the parametric model of the system. These modifications together support the hypothesis that an integrated complex mediates sensory transduction in the light responses and other responses of the sporangiophore.

INTRODUCTION

Behavioral mutants can serve as a probe of those steps of a sensory transduction chain in which they are altered. Phototropism mutants of *Phycomyces blakesleeanus* with defects in eight unlinked genes (*madA* through *madH*) have been isolated and classified genetically (Bergman et al., 1973; Ootaki et al., 1974; Eslava et al., 1976; Lipson et al., 1983; López-Díaz and Lipson, 1983). The genes *madA*, *madB*, and *madC* are associated with the photoreceptor input of the underlying sensory transduction pathway shared by phototropism, the light-growth response, and other blue-light responses. The night-blind mutants, affected in these three genes, have substantially elevated thresholds for phototropism (Bergman et al., 1973; Ootaki et al., 1974; Lipson and Terasaka, 1981; Galland and Russo, 1984*a*) but have normal gravitropism and avoidance response. In these mutants, the reduced sensitivities (increased thresholds) for phototropism are matched by corresponding reductions in sensitivity of the closely related light-growth response. Because mutants with defects in the genes *madB* and *madC* have altered photogravitropic action spectra (Galland and Lipson, 1985), the *madB* and *madC* gene products are probably part of the photoreceptor system. Mutants with defects in genes *madD* to *madG* (stiff mutants) have abnormal sporangiophore responses to light and other stimuli (namely gravity and barriers), and are thus associated with common output steps of the growth control pathways.

Unlike the mutants affected in genes *madA* to *madG*, all of which show diminished responses, the hypertropic (*madH*) mutants show enhanced tropisms to light, gravity, and barrier stimuli (Lipson et al., 1983). They also have faster adaptation kinetics (Galland and Russo, 1984*b*) and an enhanced near-ultraviolet peak in the photogravitropic action spectrum (Galland and Lipson, 1985). The *madH*-gene product apparently alters both the photoreceptor complex and the growth control output of the sensory transduction pathway. This finding suggests that the various components of the transduction pathway for phototropism and other sporangiophore responses may be organized as a molecular complex, presumably located in the plasma membrane of the sporangiophore. Recent studies with the white-noise method applied to the light-growth response of single and double *mad* mutants also support this hypothesis (Poe et al., 1986*a*, *b*).

In the previous papers (Pratap et al. 1986*a*, *b*) we have characterized the light-growth response of the wild type sporangiophore using system identification methods with sum-of-sinusoids test stimuli. In Pratap et al. (1986*a*) we derived a nonlinear model from the analysis of the frequency kernels for wild type. This model was generalized from the analytical transfer function proposed by

Address correspondence and reprint requests to Edward D. Lipson, Department of Physics, Syracuse University, Syracuse, NY 13244-1130.

Lipson (1975*a*), and consists of a nonlinear dynamic subsystem followed by a linear dynamic subsystem. The first- and second-order kernels of wild type were fit satisfactorily by this model. In Pratap et al. (1986*b*), we examined how the parameters obtained from fits of this nonlinear model to the wild-type kernels varied with wavelength and temperature. In this paper we analyze the first- and the second-order kernels of three *mad* mutants that have been associated with the photoreceptor system.

MATERIALS AND METHODS

The mutants, C109 [genotype: *madB101*(−)] (Bergman et al., 1973), L15 [genotype: *madC119 nicA101*(t)] (Lipson et al., 1980), and L85 [*madH705*(−)] (Lipson et al., 1983) were derived from the wild type NRRL1555 after mutagenesis with *N*-methyl-*N'*-nitro-*N*-nitrosoguanidine.

The experimental methods were similar to those in Pratap et al., 1986*a*. In all experiments, the wavelength of the stimulus light was 477 nm. The log-mean intensity I_0 (defined by $\log I_0 = \langle \log I \rangle$, where the angle brackets represent a time average) was chosen so that the whole range of the stimulus was above the threshold of the light-growth response for all strains studied. The night-blind mutants C109 (*madB*) and L15 (*madC*) were studied at $I_0 = 6 \times 10^{-2}$ W m^{-2}, and the hypertropic mutant L85 (*madH*) at $I_0 = 10^{-4}$ W m^{-2}. Wild-type controls were performed at both intensities.

RESULTS

Table I compares the experiments for the wild type and the three behavioral mutants. The model response (see Fig. 1 of Pratap et al., 1986*a* for definition and examples) based on the first-order kernel accounts for most of the experimental response. Of the four strains studied, the hypertropic mutant L85 (*madH*) exhibits the most nonlinear light-growth response, according to two measures. First, it shows the greatest improvement in the mean-square error (MSE) when the second-order contribution is added to the first-order model response. Secondly, the "strength of nonlinearity" (defined in Pratap et al., 1986*a*) is greatest for L85 (*madH*).

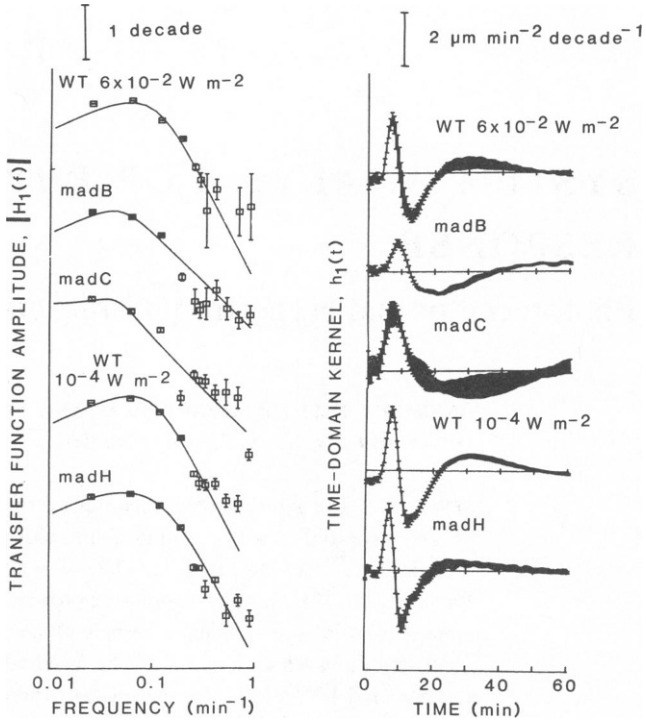

FIGURE 1 (*a*) First-order kernels in the frequency domain. The ordinate is the absolute value of the complex-valued kernel $H_1(f)$. The log-mean intensities I_0 for wild type are indicated on the figure. The log-mean intensity for C109 (*madB*) and L15 (*madC*) was $I_0 = 6 \times 10^{-2}$ W m^{-2} and for L85 (*madH*) it was $I_0 = 10^{-4}$ W m^{-2}. The experimental points are shown with error bars (standard errors for 5–6 experiments). All experiments were at wavelength 477 nm. (*b*) Time-domain kernels obtained by interpolation and Fourier transformation of the frequency-domain kernels of *a*.

The first- and second-order kernels were analyzed in terms of the internal, analytical model presented in Pratap et al. (1986*a*). The parameters were obtained from nonlinear least-squares fits of the model to the experimental kernels.

TABLE I
RESULTS OF SUM-OF-SINUSOIDS EXPERIMENTS WITH WILD TYPE AND MUTANTS

Strain	Log-mean Intensity I_0	Number of Experiments	Mean growth rate	MSE of response*			Percent improvement‡	Strength of Nonlinearity§
				Zero order	First order	Second order		
	W m^{-2}		*μm min^{-1}*	*μm^2 min^{-2}*	%	%	%	*decade^{-1}*
NRRL1555	1×10^{-4}	15	36.6 ± 2.7	41.9	30.4	15.5	49.0	0.58
NRRL1555	6×10^{-2}	7	25.9 ± 3.1	21.7	29.8	19.5	34.6	0.39
C109 (*madB*)	6×10^{-2}	6	29.9 ± 2.2	13.4	23.5	11.8	49.8	0.53
L15 (*madC*)	6×10^{-2}	6	34.4 ± 2.8	29.9	39.1	27.5	29.7	0.34
L85 (*madH*)	1×10^{-4}	7	41.1 ± 5.5	31.6	37.6	13.7	63.6	0.87

*Mean-square errors (MSE) between experimental and model response records, as described in Pratap et al., 1986*a*. The MSE for the zero-order model (h_0) is in absolute units (note: h_0 is zero because of baseline removal; therefore, the MSE of the zero-order model is simply the variance of the response after detrending). The MSEs for first-order (h_1) and second-order (h_1, h_2) models are given as percentages of zero-order MSE.

‡Percent improvement of second-order model over first-order model, i.e. the difference between the MSEs of the second- and first-order model responses as a percentage of the MSE of the first-order model response.

§Strength of nonlinearity is the ratio of the root-mean-square values of $|H_2(f_1, f_2)|$ and $|H_1(f)|$.

First-Order Kernels

The amplitude of the frequency kernel $H_1(f)$ is plotted in Fig. 1 *a* for the wild type and the three mutants. Lipson (1975*a*, *b*), who used Gaussian white noise test stimuli, determined that the power spectrum (which is theoretically equivalent in shape to the amplitude of $H_1(f)$ when both are plotted on double logarithmic scales) is approximately proportional to f at low frequency and falls off as f^{-4} at high frequency. He proposed an internal model for $H_1(f)$ that incorporated these features. That linear model is the basis for our internal model, which has been generalized to include nonlinear dynamics (Pratap et al., 1986*a*). The first-order kernel for the wild type and L85 (*madH*) are well described by this model. For C109 (*madB*) and L15 (*madC*), however, the amplitude of the kernel falls off approximately as f^{-2} at high frequencies, and the low-frequency proportionality is not discernable. The first-order kernel for these night-blind mutants has been fit accordingly to a revised model that employs only one second-order low-pass filter in the dynamic linear sybsystem instead of two.

Tables II and III present the parameters estimated from the least-squares fits of the nonlinear model developed in Pratap et al. (1986*a*) to the experimental kernels. As expected from the similarity of the wild-type first-order frequency kernels at these two intensities (Fig. 1 *a*), the parameters of the first-order model kernel (Table II) for wild type at these two intensities (10^{-4} and 6×10^{-2} W m^{-2}) are the same, within errors, except for a reduction in the gain factor at the higher intensity. The latency parameter t_0 is much larger for the *madB* mutant C109 than for wild type and the other two mutants. For C109 and for the *madC* mutant L15, the cutoff frequency of the second-order low-pass filter is smaller than for wild type. This reduction of the high-frequency cutoff (bandwidth) indicates that the *madB* and *madC* mutants have slower responses. In addition, the cutoff frequency of the first-order high-pass filter in L15 (*madC*) is shifted to lower frequency, below the resolution of the present set of experiments.

The amplitude of the frequency kernels (Fig. 1 *a*) portrays only half the information contained in the complex-valued kernels (see Pratap et al., 1986*a*). The full information is conveyed by the corresponding time-domain kernels (Fig. 1 *b*). The kernels for the hypertropic mutant and the wild-type are similar; so are the parameters derived from the frequency-domain kernels (Table II). The time-domain kernel of C109 (*madB*) shows a longer latency and is generally prolonged. The L15 (*madC*) kernel has about the same latency as the wild-type kernel, but is otherwise prolonged like the kernel of C109.

Second-Order Kernels

Figs. 2 and 3 show the amplitude of the second-order frequency kernels (*left* side) for the same set of experiments as in Fig. 1 and the corresponding model kernels (*right* side) after least-squares estimation of the parameters. Only the difference quadrant is shown, because the kernels are very small over most of the sum quadrant (see Pratap et al., 1986*a*). In the difference quadrant, these kernels are large only near the diagonal.

In Fig. 2, second-order kernels for the night-blind mutants are compared with the wild-type kernel at the same log-mean intensity (6×10^{-2} W m^{-2}). As mentioned in Pratap et al., 1986*a*, the wild-type kernel has two peaks in the difference quadrant: one at low frequencies (to the

TABLE II
FIRST-ORDER KERNEL PARAMETERS FOR WILD TYPE AND MUTANTS*

Strain	Log-mean intensity I_0	Gain factor β_L	Cutoff frequency of high-pass filter f_{L1}	Cutoff frequency of low-pass filter f_{L2}	Damping constant α_L	Latency t_0
	$W\,m^{-2}$	$\mu m\,min^{-1}\,decade^{-1}$	min^{-1}	min^{-1}		min
NRRL1555	1×10^{-4}	49.2 ± 22.0	0.063 ± 0.033	0.106 ± 0.009	0.75 ± 0.07	3.9 ± 0.1
NRRL1555	6×10^{-2}	37.1 ± 27.9	0.059 ± 0.048	0.112 ± 0.014	0.77 ± 0.08	3.7 ± 0.2
C109 (*madB*)	6×10^{-2}	22.2 ± 7.7	0.042 ± 0.019	0.050 ± 0.068	0.62 ± 0.07	6.4 ± 0.1
L15 (*madC*)	6×10^{-2}	19.2 ± 5.5	0.002 ± 0.009	0.045 ± 0.005	0.44 ± 0.16	3.8 ± 0.1
L85 (*madH*)	1×10^{-4}	12.4 ± 1.2	0.037 ± 0.031	0.153 ± 0.005	0.58 ± 0.06	4.4 ± 0.1

*Parameters for wild type and L85 (*madH*) were obtained from the nonlinear least-squares fits of the experimental first-order kernels to the following complex-valued function:

$$W(s) = \beta_L e^{-st_0}\left[\frac{s}{s + 2\pi f_{L1}}\right]\left[\frac{(2\pi f_{L2})^2}{s^2 + (2\alpha_L)(2\pi f_{L2})s + (2\pi f_{L2})^2}\right]^2,$$

where s is the Laplace transform variable, β_L the overall gain, f_{L1} the cutoff frequency of the first-order high-pass filter, f_{L2} the cutoff frequency of the second-order low-pass filter, α_L the damping constant of the low-pass filter and t_0 is the latency (see Pratap et al., 1986*a* for more complete presentation of this model, and see Fig. 4 of this paper). The subscript L indicates parameters that are part of the linear subsystem. For the mutants C109 (*madB*) and L15 (*madC*), the transfer function has only one second-order low-pass filter, i.e., the exponent of the second term of the transfer function of the wild type is unity. For all parameters, the errors represent standard errors determined from the nonlinear least-squares fitting algorithm.

TABLE III
SECOND-ORDER KERNEL PARAMETERS FOR WILD TYPE AND MUTANTS*

Strain	Log-mean intensity I_0	Gain of low-pass filter β_{N1}	Cutoff frequency of low-pass filter f_{N1}	Damping constant of low-pass filter α_{N1}	Gain of high-pass filter β_{N2}	Cutoff frequency of high-pass filter f_{N2}	Damping constant of high-pass filter α_{N2}	Exponent of high-pass filter n
	$W\,m^{-2}$	$min^{-2}\,decade^{-1/2}$	min^{-1}		$min^{-2n+1}\,decade^{-1/2}$	min^{-1}		
NRRL1555	1×10^{-4}	0.125 ± 0.003	0.032 ± 0.002	1.22 ± 0.34	0.63 ± 0.09	0.35 ± 0.02	0.183 ± 0.072	0.41 ± 0.05
NRRL1555	6×10^{-2}	0.056 ± 0.032	0.023 ± 0.002	0.97 ± 0.27	0.34 ± 0.08	0.42 ± 0.01	0.006 ± 0.011	0.32 ± 0.07
C109 (*madB*)	6×10^{-2}	0.015 ± 0.003	0.059 ± 0.002	0.24 ± 0.18	0.22 ± 0.13	0.49 ± 0.06	0.001 ± 0.002	0.63 ± 0.23
L15 (*madC*)	$6 \times 10^{+2}$	0.052 ± 0.075	0.014 ± 0.012	1.18 ± 0.64	0.40 ± 0.19	0.25 ± 0.06	0.000 ± 0.012	0.51 ± 0.31
L85 (*madH*)	1×10^{-4}	—	—	—	1.07 ± 0.08	0.08 ± 0.01	0.411 ± 0.155	0.52 ± 0.03

*The parameters were obtained by nonlinear least-squares fitting of the experimental second-order kernel to the nonlinear model developed in Pratap et al., 1986*a*. This model includes a dynamic nonlinear subsystem followed by a dynamic linear subsystem. The nonlinear subsystem includes a static squarer preceded by the sum of two linear filters (a low-pass filter and a high-pass filter):

$$P(s) = \frac{\beta_{N1}}{s^2 + (2\alpha_{N1})(2\pi f_{N1})s + (2\pi f_{N1})^2} + \frac{\beta_{N2}s}{[s^2 + (2\alpha_{N2})(2\pi f_{N2})s + (2\pi f_{N1})^2]^n},$$

where s is the Laplace transform variable, β_{N1} the gain of the low-pass filter, f_{N1} the cutoff frequency of the low-pass filter, α_{N1} the damping constant of the low-pass filter, β_{N2} the gain of the high-pass filter, f_{N2} the cutoff frequency of the high-pass filter, α_{N2} the damping constant of the high-pass filter and n the exponent of the high-pass filter. The subscript N distinguishes parameters specific for the nonlinear subsystem of the model. For L85 (*madH*) the nonlinear subsystem has only the high-pass filter, so there are no parameters for the low-pass filter.

right of the plot) and another at intermediate frequencies (near the center of the plot). The intermediate-frequency peak is larger than the low-frequency peak for wild-type, but smaller for the night-blind mutants.

The low-frequency peak for the wild-type at 6×10^{-2} W m^{-2} is at the frequency pair (0.12 min^{-1}, 0.06 min^{-1}). For the night-blind mutants, however, this maximum has been shifted to lower frequencies, and is at the frequency pair (0.03 min^{-1}, 0.06 min^{-1}). The wild-type kernel at moderate intensity (10^{-4} W m^{-2}; Fig. 3) has the low-frequency peak at (0.03 min^{-1}, 0.06 min^{-1}). Thus, with respect to the position of the low-frequency peak, the night-blind mutants at high intensity are more like wild type at moderate intensity.

The nonlinear subsystem in the internal model (see Pratap et al., 1986*a* and Fig. 4 below) includes a static squarer preceded by a dynamic linear filter (which itself is decomposed into a sum of a second-order low-pass filter, and a first-order high-pass filter). The parameters of this subsystem are given in Table III for wild type at two intensities and for the three mutants. The form of the nonlinear subsystem used for wild type describes these mutants well too. The damping constant (α_{N1}) of the second-order low-pass filter is nearly unity for wild type at both intensities and for L15; thus the filter appears to be critically damped. For C109 (*madB*) this damping constant is much smaller. In the high-pass filter, the damping constant α_{N2} is zero (within errors) for wild type at high intensity and for the night-blind mutants. The cutoff frequency f_{N2} is smaller for L15 than for C109 and wild type.

The second-order kernel for the hypertropic mutant L85 (*madH*) has an abnormal shape in the difference quadrant (Fig. 3). Unlike the wild type and the night-blind mutants, which have two peaks, the hypertropic mutant has a broad ridge-like structure along the difference diagonal. We are unable to predict the structure along the difference diagonal itself as the kernel cannot be measured there (the difference frequencies are all zero, so they all contribute to the DC level of the experimental response and cannot be separated; see Pratap et al., 1986*a*). In the sum quadrant (not shown) and away from the diagonal region in the difference quadrant, the kernel is small; the nonlinearity therefore occurs before the step that determines the cutoff frequency (bandwidth) of the system, as in the wild type (see Pratap et al., 1986*a*). The ridge-like structure does not have constant height, but has a maximum at approximately the same position as the intermediate-frequency peak in wild type; in other words, the second-order kernel for L85 appears to be missing the notch that is characteristic of wild type and the night-blind mutants.

The modified structure of the second-order kernel of the hypertropic mutant is better described by a model lacking the second-order low-pass filter in the nonlinear subsystem. The rising ridge-like structure is described well with just the high-pass filter where the cutoff frequency f_{N2} is very small, even smaller than for L15. The damping constant α_{N2} is larger for the hypertropic mutant than for the wild type and the night-blind mutants.

DISCUSSION

In this and the previous papers (Pratap et al., 1986*a*, *b*), we consider the light-growth response system to be a black box with the logarithm of light intensity as input and the change in elongation rate as the output. We have studied certain behavioral mutants to obtain further insight into the components of this black box.

The first-order kernels of two night-blind mutants, C109 (*madB*) and L15 (*madC*), were fit satisfactorily to a

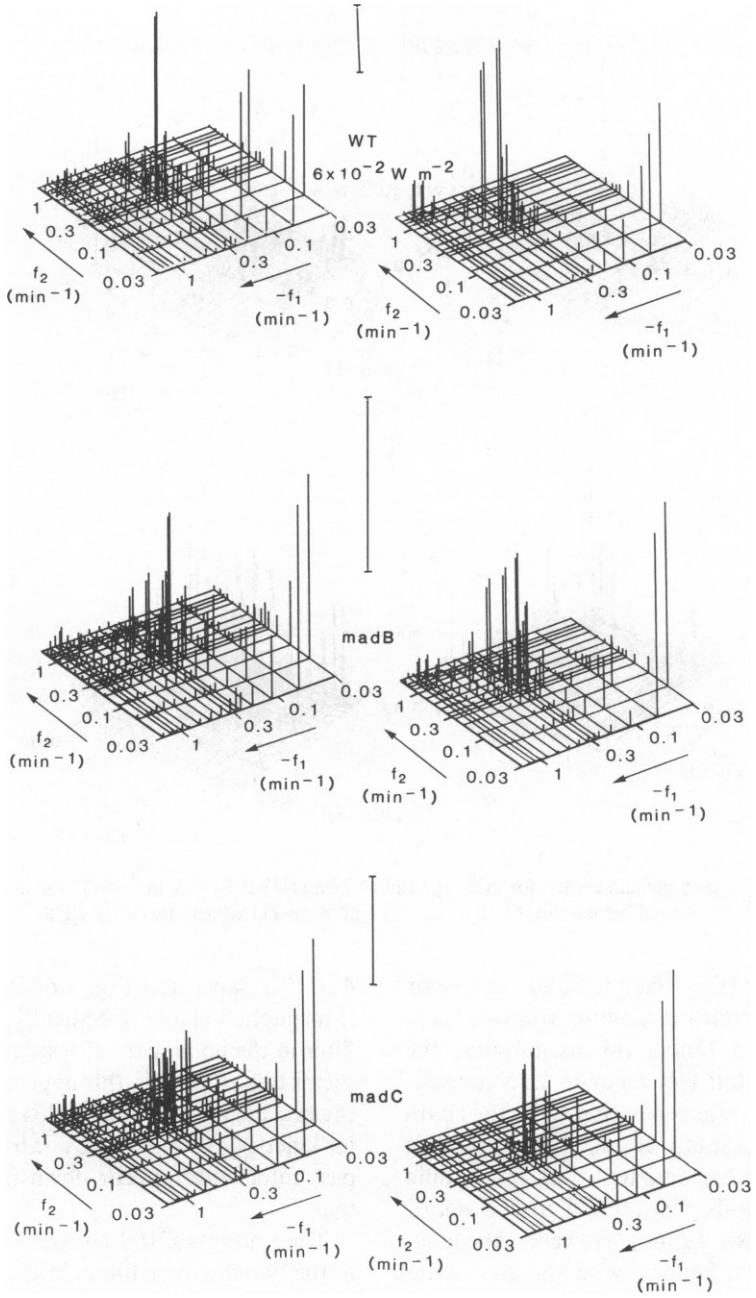

FIGURE 2 Second-order frequency-domain kernels for wild-type, C109 (*madB*) and L15 (*madC*) at 6×10^{-2} W m^{-2} of 477 nm light. The ordinate is the amplitude of the complex-valued kernel, $H_2(f_1, f_2)$. The scale bars all represent 20 μm min^{-1} decade^{-2}. The abscissae are log(f_1) and log(f_2), where f_1 and f_2 are the component frequencies in the sum-of-sinusoids stimuli. Because most of the structure is in the difference quadrant, only this quadrant is shown here. Experimental kernels plotted on the left and corresponding model kernels, calculated from fits of the model responses to the experimental responses, are plotted on the right.

reduced version of our nonlinear model (Pratap et al., 1986*a*) with just one low-pass filter in the linear subsystem instead of two. This disappearance of a low-pass filter could arise if its natural frequency were shifted (by mutation) well beyond the cutoff frequency of the system. In these mutants, the process represented by this missing second-order low-pass filter has presumably become significantly faster than the rate limiting steps in the transduction chain. In recent work with Gaussian white-noise test stimuli (Poe et al., 1986*a*) under different experimental conditions (I_0 = 0.1 W m^{-2} with broadband blue illumination), L15 (*madC*) was found to be missing one low-pass filter in the linear subsystem, and the mutant C111 (*madB*) had a significantly higher cutoff frequency of this low-pass filter.

For L15 (*madC*), at low frequency, we were unable to resolve a cutoff frequency for the high-pass filter. Lipson (1975*a*) had associated this filter with growth-rate adapta-

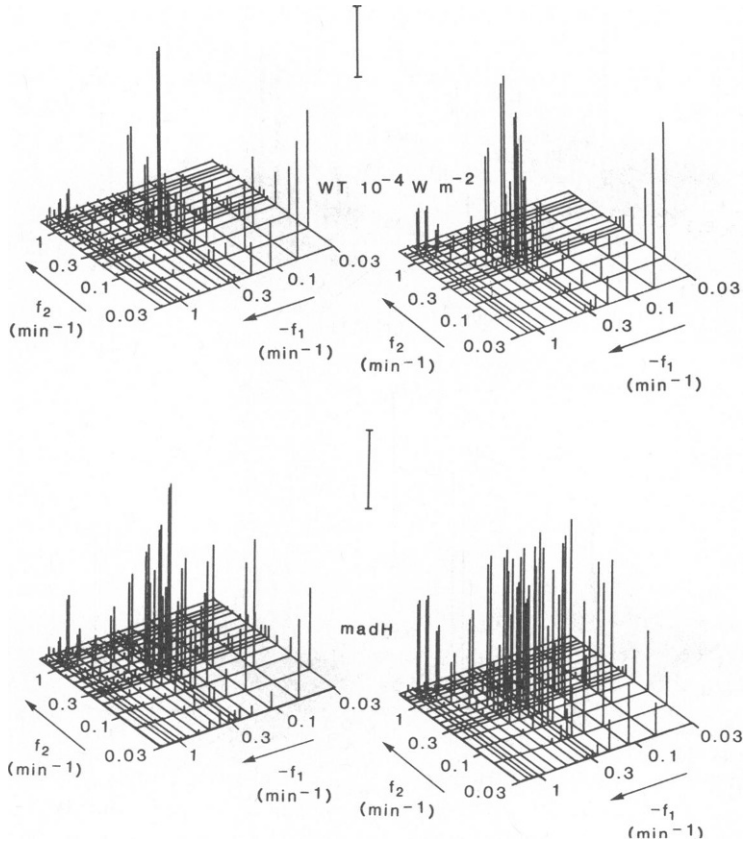

FIGURE 3 Second-order frequency-domain kernels for wild-type and L85 (*madH*) at 10^{-4} W m^{-2} of 477 nm light. The scale bars represent 20 μm min^{-1} $decade^{-2}$. The experimental kernels are shown on the left and the model kernels are on the right.

tion, because its numerator (the factor s, which represents differentiation) makes the transfer function vanish at zero frequency (i.e., $H_1(0) = 0$). Under this assumption, the very small value of this cutoff frequency in L15 suggests that the kinetics of growth-rate regulation (effector adaptation; see Discussion of Pratap et al., 1986*b*) in this mutant are very slow. This is consistent with the finding that the adaptation mechanism is altered in the *madC* mutants (Galland and Russo, 1984*b*). However, the association of the differentiation factor s with this first-order filter is arbitrary, in view of the commutativity of linear system elements. This factor could instead be associated with a second-order low-pass filter or could reasonably be left on its own to represent the fact that the response being measured is the growth rate (time derivative of growth).

The second-order kernels for the mutants and wild type share a common feature: all tend to vanish over most of the sum quadrant, and away from the diagonal in the difference quadrant. As explained in the Results section of Pratap et al., 1986*a*, this structure implies that the nonlinearity occurs before the rate-limiting step that determines the system cutoff frequency.

For the hypertropic mutant, the altered second-order kernel in the difference quadrant suggests that the mutation affects the dynamics of the nonlinear subsystem (Fig. 4 of this paper and Fig. 4 of Pratap et al., 1986*a*) of the transduction chain. Specifically, the second-order low-pass filter in the nonlinear subsystem (LP_N in Fig. 4; see below) seems to be absent in this hypertropic mutant. Presumably, the process represented by this filter has become faster and its kinetics are masked by rate-limiting steps of the low-pass filters that appear downstream in the linear subsystem.

The mutants C109 (*madB*) and L15 (*madC*) lack one of the two low-pass filters in the linear subsystem (i.e., the cutoff frequency of the missing filter has become too high to detect). The *madC* strain lacks the high-pass filter as well (i.e., the cutoff frequency of the high-pass filter has become too low to detect in our experiments). Because C109 and L15 are probable photoreceptor mutants (Galland and Lipson, 1985), the high-pass filter and one low-pass filter of the linear subsystem evidently represent processes that are associated with the photoreceptor complex. The mutant L85 (*madH*), on the other hand, is altered in the nonlinear subsystem, which lies between the logarithmic transducer and the later steps affected by *madB* and *madC* photoreceptor mutants. It seems likely then that *madH* is associated in part with the photoreceptor complex. Independent evidence that this hypertropic mutant is altered in the photoreceptor complex has

been provided by phototropic action spectra (Galland and Lipson, 1985).

Among the other parameters of the linear subsystem, the gain factor (β_L) is a product of the gains of various subsystems in cascade, and so cannot readily be localized to any particular component. Thus we would expect the overall gain to be altered in most mutants. According to studies with white-noise stimulation (R. Poe, P. Pratap, and E. Lipson, submitted for publication), the mutants affected in the genes *madA* through *madC* (input mutants) and *madD* through *madG* (output mutants) all have reduced gain. With the sum-of-sinusoids method, we too find substantially reduced gain for the night-blind mutants, and a slightly reduced gain for the hypertropic mutant.

As mentioned earlier, the mutation in gene *madH* is known to produce defects in both the input and the output parts of the transduction chain. Here we have associated the nonlinear subsystem and two filters in the linear subsystem with the photoreceptor complex. However, we have not identified any kinetic parameter of the linear subsystem that differs significantly between the hypertropic mutant and the wild type. Therefore, we are unable to detect any element in the linear subsystem that is both independent of the photoreceptor complex and altered by the hypertropic mutation.

Fig. 4 is an elaboration of the model presented in Pratap et al., 1986*a*. In this version of the model, we have indicated the sites, where the *mad* gene products appear to operate, according to the results presented in this paper. A logarithmic transducer has been added at the input (recall that the kernels were based on the logarithm of the light intensity as the input variable, under the assumption of such a transducer; see Pratap et al., 1986*a*). The *madB* and *madC* gene products are associated with this logarithmic transducer (Bergman et al., 1973), because of the pronounced elevation in their threshold for phototropism (and the light-growth response) by about 10^5-fold.

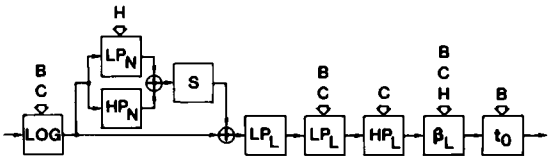

FIGURE 4 Elaboration of the analytical model for the light-growth response introduced in Pratap et al., 1986*a*. The model consists of a central linear path composed of filters, and a nonlinear feedforward path composed of linear dynamic elements and a static squarer (S). HP denotes a high-pass filter, LP a low-pass filter, β_L the overall gain, and t_0 the latency. The components of the linear path are shown with subscript L; the components of the nonlinear path are shown with subscript N. A logarithmic transducer has been included at the input. The components assumed to be affected by the different mutations are indicated by the arrows (the letters *B*, *C*, and *H* represent the genes *madB*, *madC*, and *madH*). The effects of the *B* and *C* mutations on the logarithmic transducer are according to Bergman et al. (1973).

Besides this initial action at the logarithmic transducer, the *madB* and *madC* genes influence various aspects of the dynamic linear subsystem (represented by the box *W* in Fig. 4 of Pratap et al., 1986*a*, and decomposed here as the five boxes to the right of the summing element). As mentioned before, the ordering of these linear elements is arbitrary, because of the general commutativity of linear systems. The last two boxes, which represent the overall gain factor and latency, respectively, could be decomposed further. The gain factor is a product of the gains of all of the elements. The latency too is probably distributed, in view of its wavelength dependence (Pratap et al., 1986*b*) and its alteration in the *madB* mutant. Thus the indication of effects of the mutations on these two boxes drawn at the end of the pathway should not be construed to mean that the mutations need operate at such late steps in the sensory transduction. We have deliberately placed the two filters (dynamic elements) denoted by LP_L early in the linear subsystem, because of the evidence that their defects are more closely associated with photoperception than with growth modulation (Bergman et al., 1973; Galland and Lipson, 1985; Pratap et al., 1986*b*). Although the filter HP_L is affected in the mutant L15 (*madC*), this filter is probably associated with growth regulation (Pratap et al., 1986*b*). This apparent contradiction can be resolved if one assumes that, although the gene *madC* is associated with the photoreceptors (Galland and Lipson, 1985), the photoreceptors themselves may be part of a complex that includes the growth regulation mechanism.

The hypertropic mutation acts at two sites in the scheme shown in Fig. 4. The dynamic nonlinear subsystem, just beyond the logarithmic transducer, appears to lack one of its filters (LP_N). Surprisingly, the hypertropic mutant, which shows generally enhanced tropisms, has a smaller gain factor than the wild type (Table II). Therefore, the enhanced phototropism of the *madH* mutant cannot be attributed to an enhancement of the light-growth response. This genetic distinction between the two responses supports the conclusion of Galland et al. (1985) that phototropism is not due simply to superposition of localized light-growth responses, but rather to redistribution of growth effectors.

Conclusion

The light-growth response kinetics of the *madB* and *madC* mutants differ significantly from those of the wild type. The prolonged responses of these mutants (Fig. 1) can be readily accounted for, if one assumes that they lack one of the two second-order low-pass filters present in the wild-type model. Presumably this filter is not actually deleted, but rather its cutoff frequency is elevated well beyond that of the remaining low-pass filter (i.e. well beyond the system bandwidth). On the basis of phototropic action spectra (Galland and Lipson, 1985), the *madB* and *madC* mutants have been associated with the photoreceptor complex that mediates phototropism and the light-growth response. It

seems plausible then that the kinetic steps that are altered in these mutants may reside in the photoreceptor system.

The hypertropic (*madH*) mutant exhibits only subtle changes in its light-growth response. In terms of the model (Fig. 4), this mutant is detectably altered only in the linear gain factor β_L and in the kinetics of the nonlinear subsystem. The placement of the *madH* dynamic alteration in the nonlinear subsystem (between steps that are affected by the *madB* and *madC* photoreceptor mutants) supports the hypothesis (Galland and Lipson, 1985) that the *madH* gene product not only enhances tropic responses in general but also has direct influence on the photoreceptor system.

In view of the enhanced tropisms of this hypertropic mutant, one would expect its defect to be strictly in the growth control output of the sensory transduction chain for phototropism and the light-growth response. It is surprising then that the hypertropic character also involves the photoreceptor input. One way to resolve this puzzle is to assume that there is not only a photoreceptor complex but rather there is an integrated sensory transduction complex that manages these photoresponses, as well as other responses such as gravitropism and avoidance. Comparative studies of single and double mutants by the white noise method (Poe et al., 1986*a*, *b*) provided independent evidence in support of this hypothesis.

We thank Paul Galland and Benjamin Horwitz for valuable discussions and for critical reading of the manuscript and Craig Chmielwicz for technical assistance.

This work was supported by grant GM29707 from the National Institutes of Health to Edward D. Lipson.

Received for publication 24 January 1986.

REFERENCES

Bergman, K., A. P. Eslava, and E. Cerdá-Olmedo. 1973. Mutants of *Phycomyces* with abnormal phototropism. *Mol. Gen. Genet.* 123:1–16.

Eslava, A. P., M. I. Alvarez, E. D. Lipson, D. Presti, and K. Kong. 1976. Recombination between mutants of *Phycomyces* with abnormal phototropism. *Mol. Gen. Genet.*147:235–241.

Galland, P., and E. D. Lipson. 1985. Modified action spectra of photogeotropic equilibrium in *Phycomyces* mutants with defects in genes *madA*, *madB*, *madC*, and *madH*. *Photochem. Photobiol.* 41:331–335.

Galland, P., and V. E. A. Russo. 1984*a*. Threshold and adaptation in *Phycomyces*, their interrelation and regulation by light. *J. Gen. Physiol.* 84:119–132.

Galland, P., and V. E. A. Russo. 1984*b*. Light and dark adaptation in *Phycomyces* phototropism. *J. Gen. Physiol.* 84:101–118.

Galland, P., A. Palit and E. D. Lipson. 1985. *Phycomyces*: phototropism and light-growth response to pulse stimuli. *Planta (Berl.).* 165:538–547.

Lipson, E. D. 1975*a*. White noise analysis of *Phycomyces* light growth response system. I. Normal intensity range. *Biophys. J.* 15:989–1012.

Lipson, E. D. 1975*b*. White noise analysis of *Phycomyces* light growth response system. III. Photomutants. *Biophys. J.*15:1033–1045.

Lipson, E. D. and D. T. Terasaka. 1981. Photogeotropism in *Phycomyces* double mutants. *Exp. Mycol.* 5:101–111.

Lipson, E. D., D. T. Terasaka, and P. S. Silverstein. 1980. Double mutants of *Phycomyces* with abnormal phototropism. *Mol. Gen. Genet.* 179:155–162.

Lipson, E. D., I. López-Díaz, and J. A. Pollock. 1983. Mutants of *Phycomyces* with enhanced tropisms. *Exp. Mycol.* 7:241–252.

López-Díaz, I., and E. D. Lipson. 1983. Genetic analysis of hypertropic mutants of *Phycomyces*. *Mol. Gen. Genet.* 190:318–325.

Ootaki, T., E. P. Fischer, and P. Lockhart. 1974. Complementation between mutants of *Phycomyces* with abnormal phototropism. *Mol. Gen. Genet.* 131:233–246.

Poe, R. C., P. Pratap, and E. D. Lipson. 1986*a*. System analysis of *Phycomyces* light-growth response: single mutants. *Biol. Cybern.* In press.

Poe, R. C., P. Pratap, and E. D. Lipson. 1986*b*. System analysis of *Phycomyces* light-growth response: double mutants. *Biol. Cybern.* In press.

Pratap, P., Palit, A., and Lipson, E. D. 1986*a*. System analysis of *Phycomyces* light-growth response with sum-of-sinusoids test stimuli. *Biophys. J.* 50:645–651.

Pratap, P., Palit, A., and Lipson, E. D. 1986*b*. System analysis of *Phycomyces* light-growth response. Wavelength and temperature dependence. *Biophys. J.* 50:653–660